Supporting Information

Negative Thermal Quenching One-dimensional Copper(I)-Iodide Coordination Polymer Scintillator: Enabling High-Resolution X-Ray Imaging

Zhao-Xing Gao,[a,b,c] Wen-Yan Xu ,[a,b] Wen-Fei Wang,*[d] Bao-Yi Li ,[b,c] Wen-Jing Jiang,[c] Shuai-Hua Wang ,[b,c] Fa-Kun Zheng ,*[b,c] and Guo-Cong Guo*[b]

[a]College of Chemistry, Fuzhou University, Fuzhou, Fujian 350108, P. R. China

[b]State Key Laboratory of Structural Chemistry, Fujian Institute of Research on the Structure of Matter, Chinese Academy of Sciences, Fuzhou, Fujian 350002, P. R. China

[c]Fujian Science & Technology Innovation Laboratory for Optoelectronic Information of China, Fuzhou, Fujian 350108, P. R. China

[d]College of Chemistry and Chemical Engineering, Qingdao University, Qingdao, Shandong 266071, P. R. China

* Corresponding author to E-mail: wangwenfei2@qdu.edu.cn; zfk@fjirsm.ac.cn; gcguo@ fjirsm.ac.cn

Supplementary figures

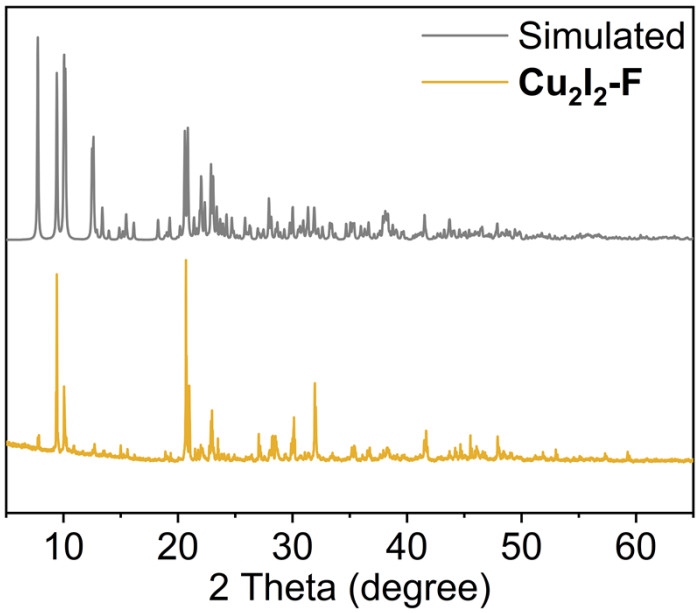

Figure S1. PXRD patterns of **Cu_2I_2-F**.

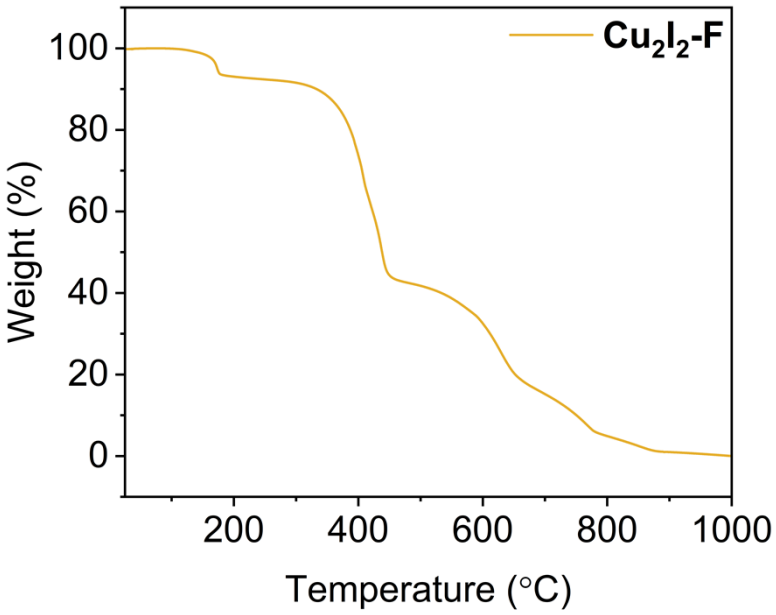

Figure S2. TGA curve for **Cu_2I_2-F**.

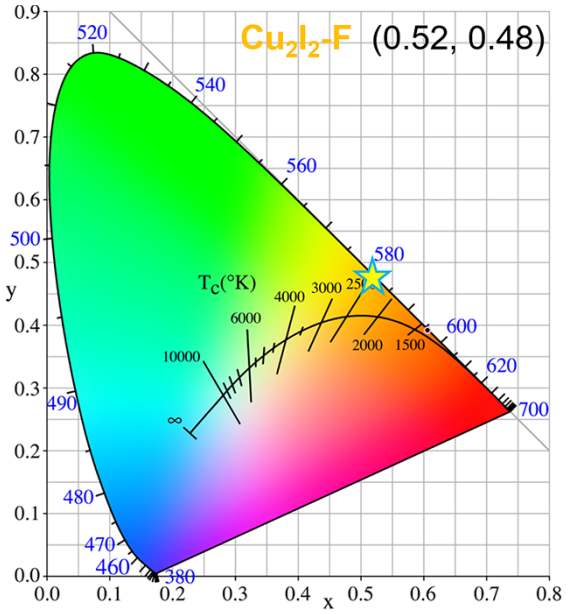

Figure S3. Commission Internationale de l'Eclairage (CIE) chromaticity coordinate diagram of the photoluminescence of the solid **Cu_2I_2-F**.

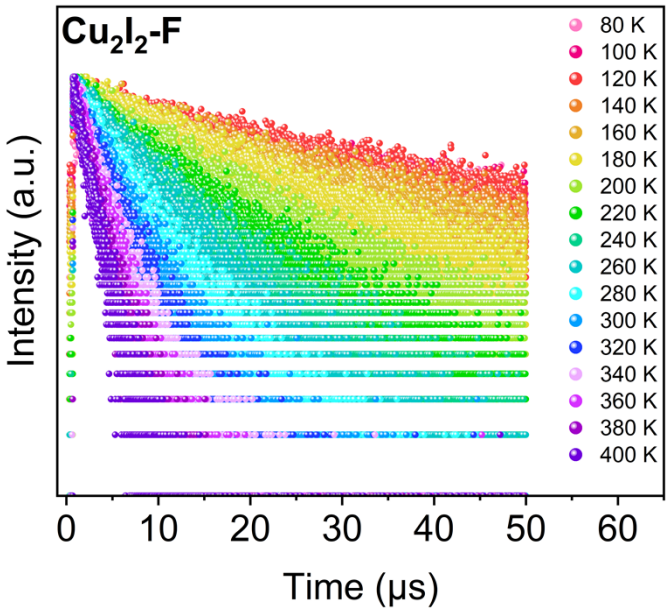

Figure S4. Temperature-dependent time-resolved PL decay of **Cu_2I_2-F**.

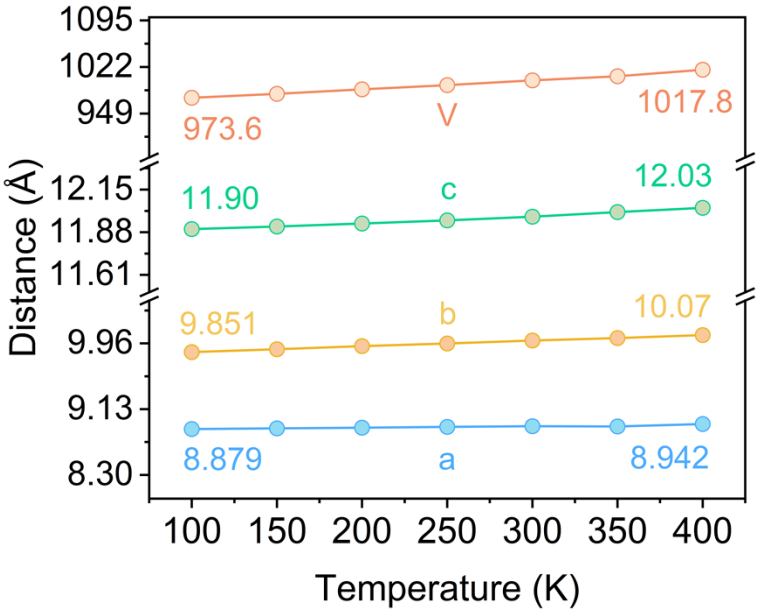

Figure S5. Temperature-dependent cell parameters of **Cu_2I_2-F**.

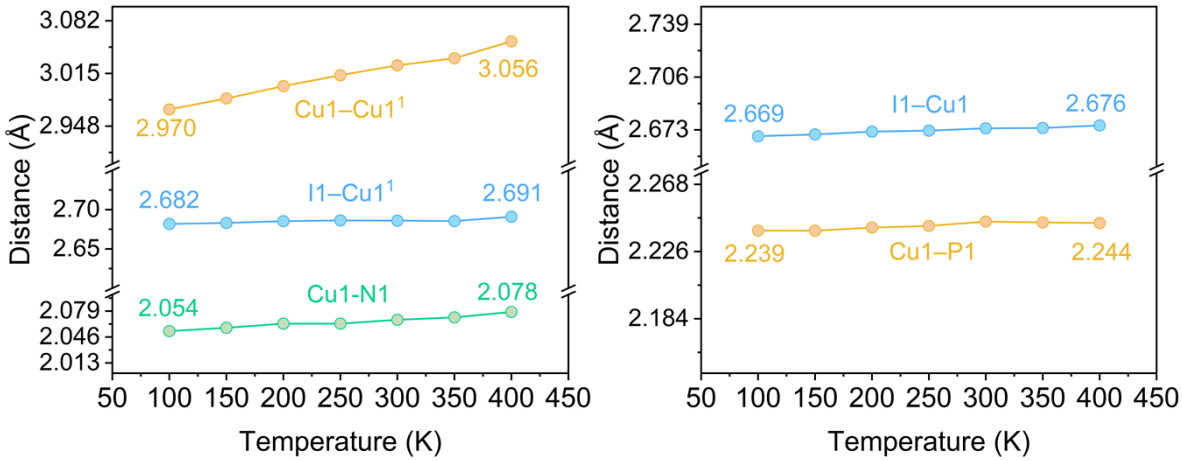

Figure S6. Temperature-dependent Cu···Cu distances and selected bond lengths in **Cu_2I_2-F**.

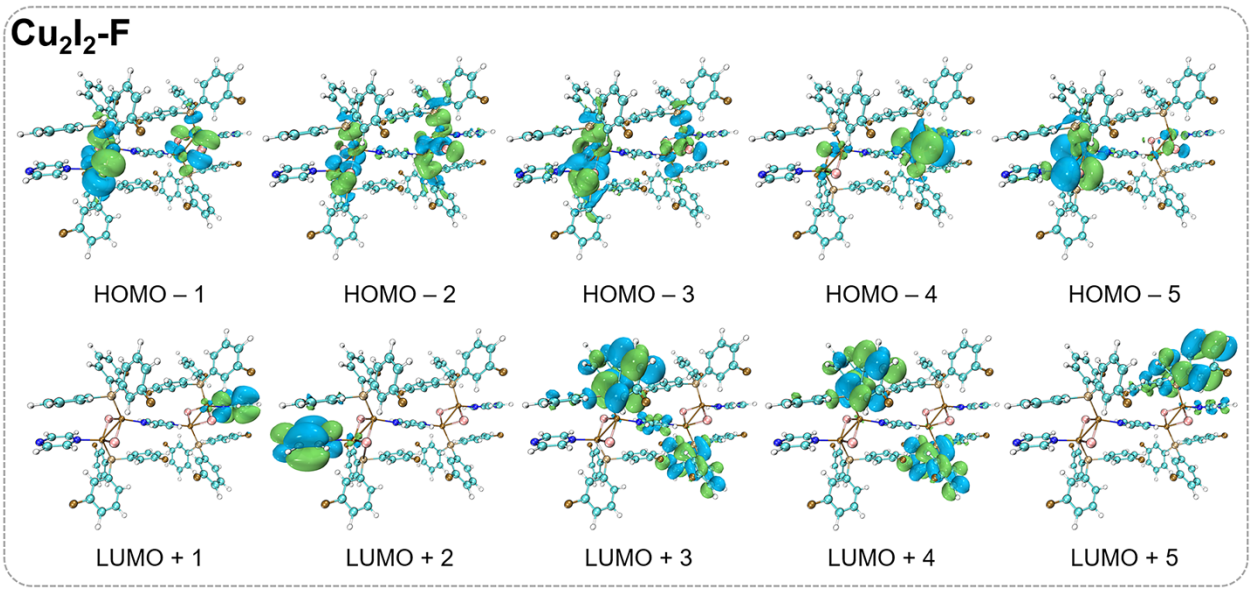

Figure S7. The calculated frontier orbitals of **Cu_2I_2-F**.

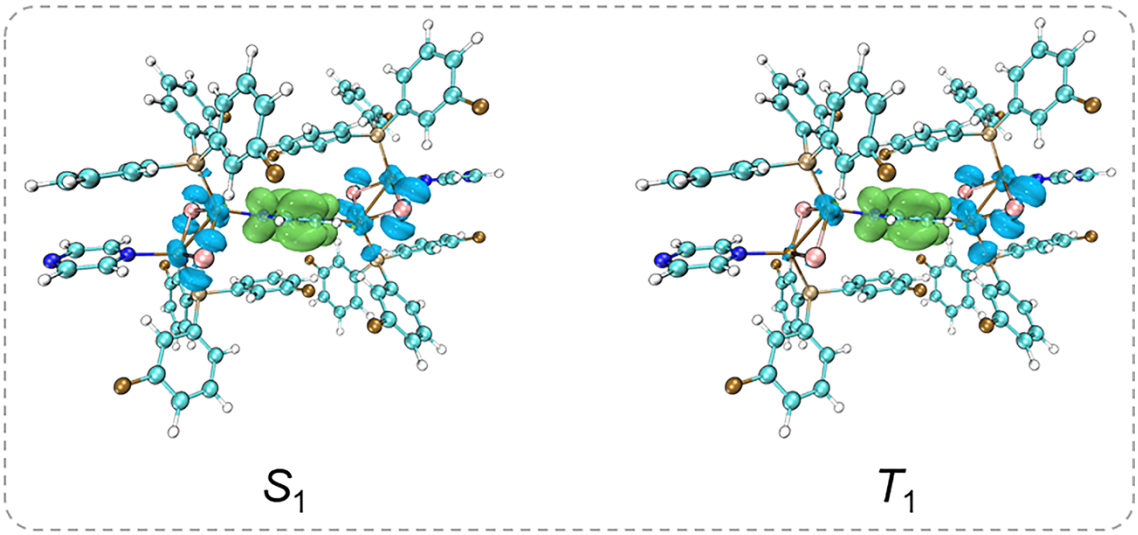

Figure S8. CDD maps of S_1 and T_1 states for **Cu_2I_2-F**.

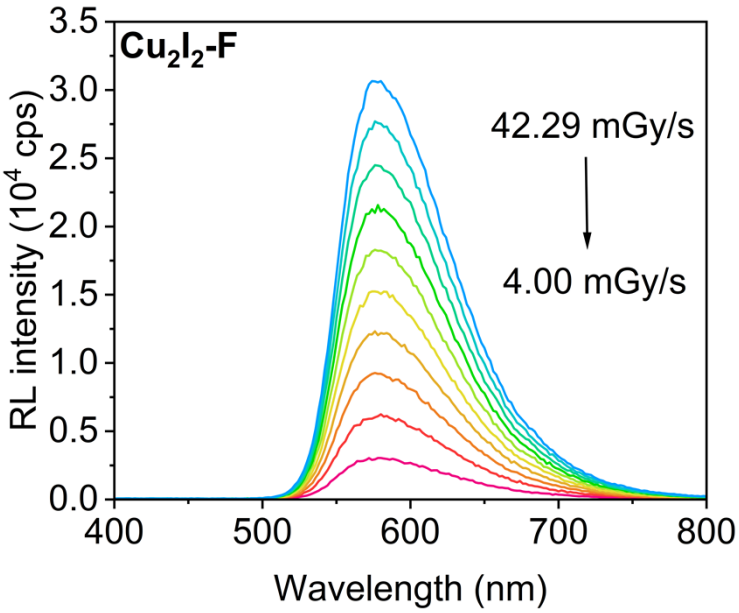

Figure S9. The X-ray dose rate-dependent RL spectra of **Cu_2I_2-F**.

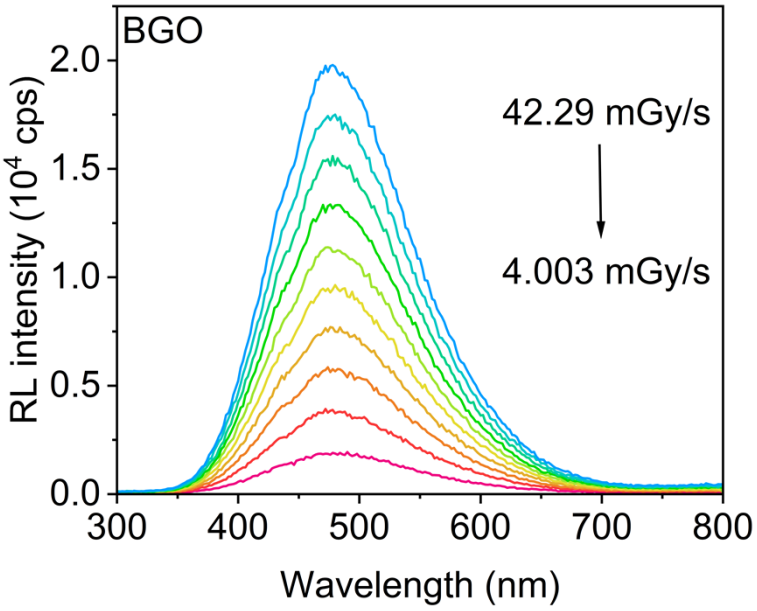

Figure S10. The X-ray dose rate-dependent RL spectra of BGO.

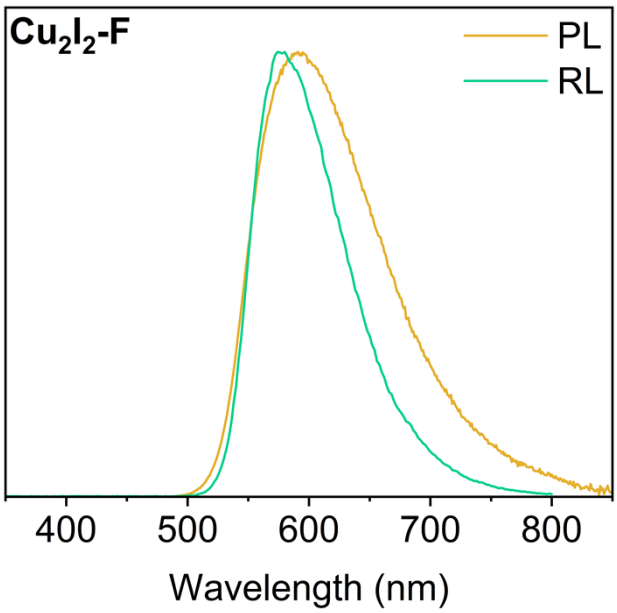

Figure S11. Comparison of PL and RL emission spectra of **Cu_2I_2-F**.

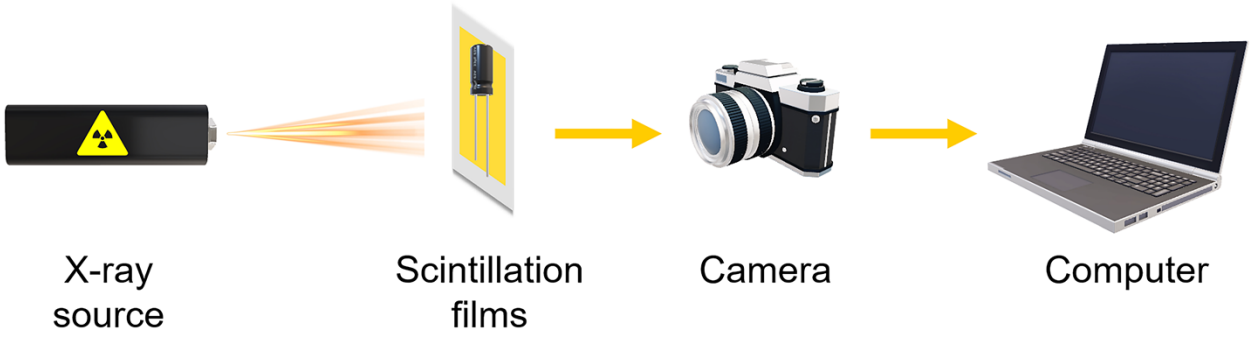

Figure S12. Schematic diagram of the experimental setup utilized for X-ray imaging.

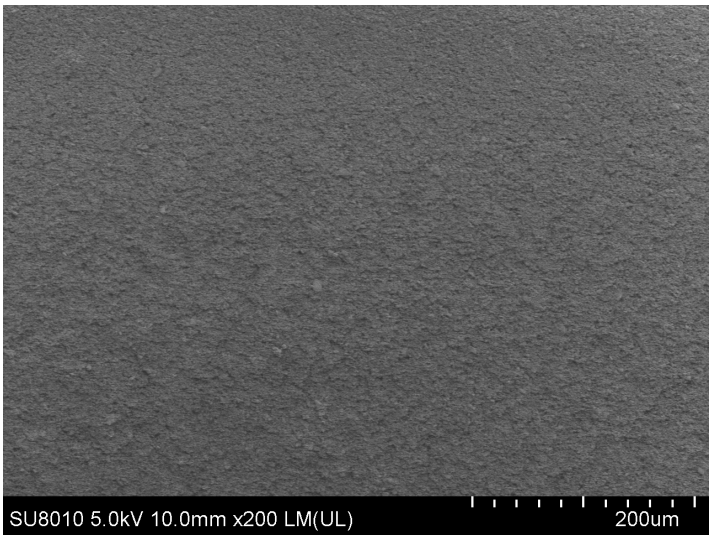

Figure S13. SEM imaging of the **Cu_2I_2-F**-film.

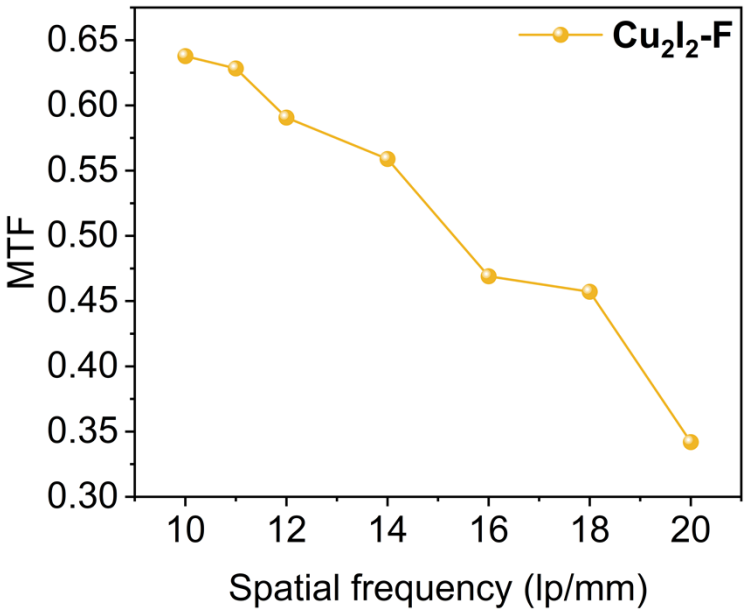

Figure S14. The MTF value of the **Cu_2I_2-F**-film by the line-pair pattern method.

Supplementary tables

Table S1. Crystal data and structure refinement of **Cu_2I_2-F**.

Compound	**Cu_2I_2-F**
CCDC	2515892
Formula	$C_{40}H_{28}Cu_2F_6I_2N_2P_2$
M_r	1093.46
T/K	300
Crystal system	triclinic
Space group	*P-1*
a/Å	8.91430(10)
b/Å	9.99620(10)
c/Å	11.9783(2)
α/°	71.9450(10)
β/°	89.0310(10)
γ/°	80.7840(10)
V [Å^3]	1001.11(2)
Z	1
Calcd. density (g cm^{-3})	1.814
μ/mm^{-1}	2.744
F(000)	530.0
2*θ* [deg]	3.578 to 53.668
Reflections collected	19500
Goodness-of-fit on F^2	1.045
Final *R* indices [$I > 2\sigma(I)$]	$R_1 = 0.0282$ $wR_2 = 0.0678$

[a]$R_1 = \sum(F_o - F_c)/\sum F_o$. [b]$wR_2 = [\sum w(F_o^2 - F_c^2)^2/\sum w(F_o^2)^2]^{1/2}$.

Table S2. Bond lengths (Å) and bond angles (º) of **Cu_2I_2-F** at 300 K.

Selected bond lengths (Å)			
I1–Cu1	2.6740(4)	Cu1–P1	2.2447(8)
I1–Cu1[1]	2.6859(4)	Cu1–N1	2.068(2)
Cu1–Cu1[1]	3.0253(7)		
Selected bond angles (º)			
Cu1–I1–Cu1[1]	68.725(14)	N1–Cu1–I1	106.34(6)
I1–Cu1–I1[1]	111.275(14)	N1–Cu1–Cu1[1]	120.11(7)
I1[1]–Cu1–Cu1[1]	55.452(13)	N1–Cu1–P1	122.37(7)
I1–Cu1–Cu1[1]	55.823(12)	C3–P1–Cu1	117.12(11)
P1–Cu1–I1	105.59(2)	C9–P1–Cu1	117.11(11)
P1–Cu1–I1[1]	104.65(2)	C15–P1–Cu1	110.86(10)
P1–Cu1–Cu1[1]	117.52(3)	C2–N1–Cu1	122.7(2)
N1–Cu1–I1[1]	106.56(7)	C1–N1–Cu1	121.7(2)

Symmetric code: [1] $1 - x, 2 - y, -z$

Table S3. Crystal data and structure refinement of **Cu_2I_2-F** at different temperatures (100–400 K).

Temperature	100 K	150 K	200 K
Formula	$C_{40}H_{28}Cu_2F_6I_2N_2P_2$	$C_{40}H_{28}Cu_2F_6I_2N_2P_2$	$C_{40}H_{28}Cu_2F_6I_2N_2P_2$
M_r	1093.46	1093.46	1093.46
Crystal system	triclinic	triclinic	triclinic
Space group	*P-1*	*P-1*	*P-1*
a/Å	8.87940(10)	8.88710(10)	8.8964(2)
b/Å	9.85130(10)	9.8865(2)	9.9262(2)
c/Å	11.8999(2)	11.9162(2)	11.9355(3)
α/°	108.6070(10)	71.5110(10)	71.644(2)
β/°	90.1600(10)	89.9350(10)	89.677(2)
γ/°	98.7280(10)	81.1380(10)	80.997(2)
V [Å^3]	973.64(2)	979.82(3)	986.97(4)
Z	1	1	1
Calcd. density (g cm^{-3})	1.865	1.853	1.840
μ/mm^{-1}	2.821	2.803	2.783
F(000)	530.0	530.0	530.0
2θ [deg]	3.616 to 60.706	3.608 to 60.986	3.6 to 60.692
Reflections collected	22262	22436	22178
Goodness-of-fit on F^2	1.054	1.051	1.049
Final R indices [$I > 2\sigma(I)$]	$R_1 = 0.0258$ $wR_2 = 0.0579$	$R_1 = 0.0281$ $wR_2 = 0.0605$	$R_1 = 0.0312$ $wR_2 = 0.0694$

[a]$R_1 = \sum(F_o - F_c)/\sum F_o$. [b]$wR_2 = [\sum w(F_o^2 - F_c^2)^2/\sum w(F_o^2)^2]^{1/2}$.

Temperature	250 K	300 K	350 K	400 K
Formula	$C_{40}H_{28}Cu_2F_6I_2N_2P_2$	$C_{40}H_{28}Cu_2F_6I_2N_2P_2$	$C_{40}H_{28}Cu_2F_6I_2N_2P_2$	$C_{40}H_{28}Cu_2F_6I_2N_2P_2$
M_r	1093.46	1093.46	1093.46	1093.46
Crystal system	triclinic	triclinic	triclinic	triclinic
Space group	*P-1*	*P-1*	*P-1*	*P-1*
a/Å	8.90700(10)	8.91430(10)	8.9123(4)	8.9421(4)
b/Å	9.9592(2)	9.99620(10)	10.0282(6)	10.0653(6)
c/Å	11.9549(2)	11.9783(2)	12.0080(8)	12.0343(8)
α/°	71.765(2)	71.9450(10)	72.114(5)	72.297(5)
β/°	89.3610(10)	89.0310(10)	88.671(4)	88.128(4)
γ/°	80.8630(10)	80.7840(10)	80.686(4)	80.587(4)
V [Å^3]	993.60(3)	1001.11(2)	1007.47(11)	1017.79(11)
Z	1	1	1	1
Calcd. density (g cm^{-3})	1.827	1.814	1.802	1.784
μ/mm^{-1}	2.764	2.744	2.726	2.699
F(000)	530.0	530.0	530.0	530.0
2θ [deg]	3.59 to 60.926	3.578 to 53.668	3.566 to 55.122	3.554 to 55.194
Reflections collected	22804	19500	19349	19575
Goodness-of-fit on F^2	1.040	1.045	1.040	1.064
Final R indices	$R_1 = 0.0334$	$R_1 = 0.0282$	$R_1 = 0.0299$	$R_1 = 0.0317$
[$I > 2\sigma(I)$]	$wR_2 = 0.0723$	$wR_2 = 0.0678$	$wR_2 = 0.0787$	$wR_2 = 0.0862$

[a]$R_1 = \sum(F_o - F_c)/\sum F_o$. [b]$wR_2 = [\sum w(F_o^2 - F_c^2)^2/\sum w(F_o^2)^2]^{1/2}$.

Table S4. Cu···Cu distances and selected bond lengths (Å) of **Cu_2I_2-F** at different temperatures (100–400 K).

Temperature	100 K	150 K	200 K	250 K
I1–Cu1	2.6691(3)	2.6702(3)	2.6719(4)	2.6726(4)
I1–Cu1[1]	2.6817(3)	2.6830(3)	2.6853(4)	2.6862(4)
Cu1–Cu1[1]	2.9693(6)	2.9833(6)	2.9989(6)	3.0128(7)
Cu1–P1	2.2391(7)	2.2390(7)	2.2410(7)	2.2420(8)
Cu1–N1	2.0535(19)	2.0578(19)	2.063(2)	2.063(2)
Temperature	300 K	350 K	400 K	
I1–Cu1	2.6740(4)	2.6742(4)	2.6758(5)	
I1–Cu1[1]	2.6859(4)	2.6854(5)	2.6909(5)	
Cu1–Cu1[1]	3.0253(7)	3.0343(7)	3.0559(8)	
Cu1–P1	2.2447(8)	2.2442(8)	2.2438(9)	
Cu1–N1	2.068(2)	2.071(2)	2.078(2)	

Symmetric codes: [1] $1 - x, 2 - y, -z$